

Theoretical Accuracy Analysis of RSS-Based Range Estimation for Visible Light Communication

Changeez Amini^a, Paeiz Azmi^{a,*}, Seyed Sadra Kashef^b

^a*Department of Electrical and Computer Engineering, Tarbiat Modares University, Tehran, Iran.*

^b*Department of Electrical and Computer Engineering, Urmia University, Urmia, Iran.*

Abstract

In this paper, an improved channel model of visible light communication (VLC) for ranging is presented. For indoor channel model of VLC, distance is estimated based on received signal strength. In this model, received shot noise as a distance dependent parameter is considered in range estimation accuracy. Moreover, based on this model, the Cramer-Rao lower bound is computed as the theoretical limits on the performance and accuracy of any unbiased estimator. In this way, the effects of horizontal and vertical distances are investigated. In addition, the transmitted power effect on RSN and accordingly on CRLB is demonstrated.

Keywords: Visible light communication, range estimation, received shot noise, Cramer-Rao lower bound.

1. Introduction

Recently, visible light communication (VLC) has gradually become a research hotspot in indoor environments because of its advantages such as illumination and a high capacity for data transmission [1]. Additionally, the optical communication systems are safe where radio frequency (RF) is hazardous or even forbidden (same as underground mines, airplanes, submarines, intrinsically safe environments like petrochemical industries and so on). Also, the radio

*Corresponding author

Email addresses: c.amini@modares.ac.ir (Changeez Amini), pazmi@modares.ac.ir (Paeiz Azmi), s.kashef@urmia.ac.ir (Seyed Sadra Kashef)

wave is more vulnerable to multipath effects than visible light. Furthermore, the light-emitting diode (LED) based localization is a promising approach as it can provide highly accurate positioning, inexpensively. Within the last years, increasing research in visible light positioning (VLP) can be observed which can make VLC as a more practical technology. The VLP systems use the photodiode (PD), extracting features from the received signals such as received signal strength (RSS), angle of arrival (AOA), time of arrival (TOA), and time difference of arrival (TDOA) [2, 3, 4, 5]. By using the least-squares method, the accuracy of indoor visible light communication localization system based on RSS in non-line-of-sight environments is analyzed in [6]. In [7], the authors have investigated the simultaneous position and orientation estimation problem using RSS. Cramer-Rao lower bound (CRLB) as a fundamental limit on RSS based range estimation is investigated in [8]. In [9], the CRLB of the position error is determined using RSS measurements. It is demonstrated in [10] that RSS-based distance estimation in VLP is biased. In [11], a low-complexity TDOA-based VLP system using a novel and practical localization scheme based on cross-correlation has been proposed and experimentally demonstrated. Performance improvements over AOA based positioning are illustrated by simulation in which combines AOA and RSS information to enhance positioning accuracy in an asynchronous VLP system [12]. Moreover, [13] applies the phase difference of arrival (PDOA) as the optical wireless positioning technique.

Generally, four noise sources are considered in VLP, which are thermal noise, shot noise of background radiation, shot noise of dark current and shot noise of received signal (RSN). The total effect of these four noises is integrated as a total noise. It is assumed that the total noise has Gaussian probability distribution function (p.d.f.) and the variance of this noise equals to the sum of the variance of four noise sources. [14]. Note that the first three noise sources are constant respect to the received signal power transmitted by LED and received in the photodetector. However, opposite to other noise sources, RSN depends on received signal power and range of receiver from the transmitter. Dependence of RSN variance to the distance affects the total noise variance considerably

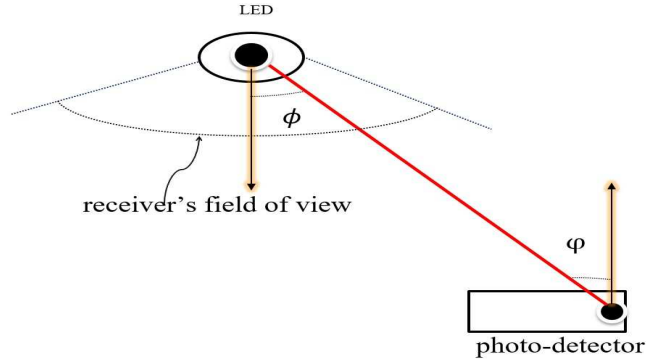


Figure 1: Two-dimensional schematic figure of the geometry of the LED source and photo-detector (receiver) in the VLC system. LOS path is the main path from the optical power source to the receiver.

which can increase $\sqrt{\text{CRLB}}$ in RSS. Whereas it is shown in other fields such as channel capacity [15, 16] that the effect of input-dependent Gaussian noise (RSN) can not be ignored, this effect has not been considered so far in VLP to the best of our knowledge.

In this letter, CRLB is calculated theoretically by taking into account received signal power-dependent RSN. In this way, the effects of horizontal and vertical distances are investigated. In addition, the transmitted power effect on RSN and accordingly on CRLB is demonstrated. The rest of the paper is organized as follows: in Section 2, we describe the system model and present the basic assumptions. In Section 3, we derive the exact closed-form expression for the CRLB. Simulations and related discussions are given in Section 4. Finally, conclusions are drawn in Section 5.

2. System Model and Basic Assumptions

We suppose a VLC system with the corresponding transmitter and receiver. Let ϕ be the angle of irradiance respect to the normal axis of transmitter surface and φ be the angle of incidence respect to the normal axis of desk plane. Angles ϕ and φ are associated with the locations of the LED source and the receiver.

In this case, the channel LOS gain is given by

$$\eta_{\text{LOS}} = \begin{cases} \frac{(m+1)S}{2\pi d^2} \cos^m \phi T_s(\varphi) g(\varphi) \cos \varphi, & 0 \leq \varphi \leq \varphi_{\text{con}} \\ 0, & \varphi > \varphi_{\text{con}} \end{cases}, \quad (1)$$

where m is the order of Lambertian emission, S is the active area of the detector, and d denotes the distance between transmitter and the receiver surface. φ_{con} is the field of view (FOV) of the receiver. $T_s(\varphi)$ and $g(\varphi)$ are the gain of the optical filter and the gain of the optical concentrator, respectively. For sake of simplicity, the parameters are assumed such that $T_s(\varphi) = g(\varphi) = 1$ [17].

In general, the multipath transmission in VLC is not challenging like RF. Typically, the power of the reflected components will be much lower than LOS path [18]. The channel gain is almost flat and the received power is given by the channel DC gain on the directed path and diffuse links [19]. The channel gain is given by

$$H(0) = \eta_{\text{LOS}} + \eta_{\text{diff}}, \quad (2)$$

where η_{diff} expresses the channel diffuse gain. Thus the received optical power can be summarized by

$$x = R_p H(0) P_t + w = P_0 + P_{\text{diff}} + w, \quad (3)$$

where $P_0 = R_p \eta_{\text{LOS}} P_t$ and $P_{\text{diff}} = R_p \eta_{\text{diff}} P_t$. w is additive white Gaussian noise (AWGN) and R_p denotes the detector responsivity. P_t denotes the transmitted optical power. In practice, eye safety limitations impose a fundamental constraint on the P_t .

Figure 1 illustrates the geometry of an indoor VLC system with one LED lamp located on the ceiling. The receiver has a sensor which estimates the distance between itself and the transmitter based on the measured RSS. Generally, in the VLC systems, the receiver is pointed straight up at the ceiling and the transmitter is pointed straight down from the ceiling and it is placed within the receiver-field of view. As a result, $\cos \phi = \cos \varphi = \frac{h}{d}$ and the LOS power can be expressed as

$$P_0 = R_p P_t \frac{(m+1)S}{2\pi} \frac{h^{m+1}}{d^{m+3}}, \quad (4)$$

where vertical distance is represented by h . Based on diffuse links considered in [20], the influence to CRLB of multipath reflections is ignorable when diffuse channel gain has already been measured in a specific scenario and the modulation speed is much slower than the channel cut-off frequency. Thus, η_{diff} can be treated as a constant.

In the visible light system, the noise model could be separated into several sources as follows [21]:

1) *Thermal Noise* σ_{TH} : The thermal (Johnson) noise is given as $\sigma_{TH} = \sqrt{\frac{8\pi\kappa T_e}{G}\eta SI_2 B^2 + \frac{16\pi^2\kappa T_e\Gamma}{g_m}\eta^2 S^2 I_3 B^3}$, where k denotes the Boltzmann constant, T_e represents the absolute temperature, G is the open-loop voltage gain, η is the fixed capacitance of photodetector per unit area, Γ is the channel noise factor, B is the equivalent noise bandwidth, g_m is the transconductance, and the noise bandwidth factors are $I_2 = 0.562$ and $I_3 = 0.0868$.

2) *Shot Noise From Background Radiation* σ_{BG} : The current noise from background radiation is $\sigma_{BG} = \sqrt{2qR_p p_{BS} S \check{\lambda} B}$, where q is the electron charge, p_{BS} is the background spectral irradiance, $\check{\lambda}$ is the bandwidth of the optical filter.

3) *Shot Noise From Dark Current* σ_{DC} : The noise from the dark current of a photodiode is $\sigma_{DC} = \sqrt{2qI_{DC}B}$, where I_{DC} refers to the photodiode dark current.

4) *RSN* σ_{SS} : The shot noise can be expressed as $\sigma_{SS} = \sqrt{2q(P_0 + P_{\text{diff}})B}$. Clearly, RSN depends on LOS power. Nevertheless, RSN is supposed to be constant in previous VLP works to the best of our knowledge.

Thus the variance of Gaussian noise detected by the receiver can be summarized by

$$\sigma_0^2 = \sigma_{TH}^2 + \sigma_{BG}^2 + \sigma_{DC}^2 + \sigma_{SS}^2 = \sigma_T^2 + \sigma_{SS}^2. \quad (5)$$

One can find a detailed discussion about noise sources and an in-depth analysis of their influence on the signal-to-noise ratio (SNR) in [22].

3. Cramer-Rao Lower Bound

In this part, theoretical limits on ranging accuracy are investigated by deriving the CRLB for the provided model. Note that RSS can estimate only one parameter, so it is assumed that vertical distance (height) is known which is a common assumption [20]. First, we write the probability density function (PDF) of the received optical power using Equation (3) as

$$p(x; d) = \frac{1}{\sigma_0 \sqrt{2\pi}} \exp \left\{ -\frac{1}{2\sigma_0^2} (x - P_0 - P_{\text{diff}})^2 \right\}, \quad (6)$$

By using the natural logarithm, we have

$$\ln p(x; d) = -\ln \sigma_0 \sqrt{2\pi} - \frac{1}{2\sigma_0^2} (x - P_0 - P_{\text{diff}})^2. \quad (7)$$

Differentiating the log-likelihood function, we have

$$\frac{\partial \ln p(x; d)}{\partial d} = -\frac{\frac{\partial \sigma_0}{\partial d}}{\sigma_0} + \frac{\frac{\partial \sigma_0}{\partial d}}{\sigma_0^3} (x - P_0 - P_{\text{diff}})^2 + \frac{1}{\sigma_0^2} (x - P_0 - P_{\text{diff}}) \frac{\partial P_0}{\partial d}, \quad (8)$$

concerning the relationship between the RSN and the received optical power, $\frac{\partial \sigma_0}{\partial d}$ is equal to

$$\frac{\partial \sigma_0}{\partial d} = qB(\sigma_T^2 + 2q(P_0 + P_{\text{diff}})B)^{-\frac{1}{2}} \frac{\partial P_0}{\partial d} = \frac{qB}{\sigma_0} \frac{\partial P_0}{\partial d}. \quad (9)$$

Alternatively, by using Equation (9), we can rewrite Equation (8) as

$$\frac{\partial \ln p(x; d)}{\partial d} = -\frac{qB}{\sigma_0^2} \frac{\partial P_0}{\partial d} + \frac{qB}{\sigma_0^4} (x - P_0 - P_{\text{diff}})^2 \frac{\partial P_0}{\partial d} + \frac{1}{\sigma_0^2} (x - P_0 - P_{\text{diff}}) \frac{\partial P_0}{\partial d}. \quad (10)$$

By using Equation (9), the second derivative would be

$$\begin{aligned} \frac{\partial^2 \ln p(x; d)}{\partial d^2} &= \frac{2(qB)^2}{\sigma_0^4} \left(\frac{\partial P_0}{\partial d} \right)^2 - \frac{qB}{\sigma_0^2} \frac{\partial^2 P_0}{\partial d^2} - 4 \frac{(qB)^2}{\sigma_0^6} (x - P_0 - P_{\text{diff}})^2 \left(\frac{\partial P_0}{\partial d} \right)^2 \\ &\quad - \frac{2qB}{\sigma_0^4} (x - P_0 - P_{\text{diff}}) \left(\frac{\partial P_0}{\partial d} \right)^2 + \frac{qB}{\sigma_0^4} (x - P_0 - P_{\text{diff}})^2 \frac{\partial^2 P_0}{\partial d^2} \\ &\quad - 2 \frac{qB}{\sigma_0^4} (x - P_0 - P_{\text{diff}}) \left(\frac{\partial P_0}{\partial d} \right)^2 - \frac{1}{\sigma_0^2} \left(\frac{\partial P_0}{\partial d} \right)^2 + \frac{1}{\sigma_0^2} (x - P_0 - P_{\text{diff}}) \frac{\partial^2 P_0}{\partial d^2}. \end{aligned} \quad (11)$$

Upon taking the negative expected value we have

$$-\mathbb{E} \left[\frac{\partial^2 \ln p(x; d)}{\partial d^2} \right] = \left(\frac{\partial P_0}{\partial d} \right)^2 \left[\frac{2(qB)^2}{\sigma_0^4} + \frac{1}{\sigma_0^2} \right]. \quad (12)$$

Then, the variance of any unbiased estimator must satisfy

$$\sqrt{\text{var}(\hat{d}_0)} \geq \sqrt{\frac{1}{\sigma_0^2 + 2(qB)^2} \frac{\sigma_0^2}{|\frac{\partial P_0}{\partial d}|}}, \quad (13)$$

where $|\frac{\partial P_0}{\partial d}|$ refers to absolute value of $\frac{\partial P_0}{\partial d}$ which is given by

$$\frac{\partial P_0}{\partial d} = -\frac{R_p P_t S}{2\pi} (m+1)(m+3) \frac{h^{m+1}}{d^{m+4}}. \quad (14)$$

4. Numerical Results and Discussion

In this section, the simulation results are provided to evaluate the performance of the RSS method. The CRLB results (by taking account of the impact of the channel DC gain, as well as the RSN,) are simulated and studied in this section. The simulations parameters are listed in Table 1.

By considering the RSN, the Gaussian noise variance consists of a constant parameter (σ_T^2) and a variable one (σ_{SS}^2). According to the parameters of Table 1, we can calculate $\sigma_{TH}^2 = 1.12 \cdot 10^{-13}$, $\sigma_{BG}^2 = 2.38 \cdot 10^{-14}$, and $\sigma_{DC}^2 = 6.40 \cdot 10^{-22}$ which in total is $\sigma_T^2 = 1.36 \cdot 10^{-13}$. The value of m can be expressed as $m = -\frac{\ln 2}{\ln(\theta_{\frac{1}{2}})}$, where $\theta_{\frac{1}{2}}$ is defined as the view angle when irradiance is half of the value at 0° . When the value of m increases, it means the value of $\theta_{\frac{1}{2}}$ decreases. The signal is more concentrated and the SNR is higher. Therefore, the accuracy is higher. By considering this fact, CRLB is plotted in [20] versus source optical power with several numbers of m . The effect of the variable parameter is shown in Fig. 2 which is a contour plot under the three-dimensional shaded surface where $m = 50$, and $P_t = 1W$. Obviously, the effect of the RSN is mainly visible just below the LED, while further away (horizontally) from the LED, the effect is diminishable. Although, because of benefits provided by higher SNRs, it is more likely to utilize the receiver near to the transmitter. If so, RSN (σ_{SS}^2) is not negligible and has a noticeable effect on the analysis of indoor VLC system.

In Fig. 3, the effect of distance over $\sqrt{\text{CRLB}}$ is shown where it is assumed $m = 1$, $P_t = 1W$. ℓ refers to the horizontal distance between the transmitter

Table 1: Some typical parameter values

Parameter	Value
Electron Charge (q)	1.6×10^{-19} C
Dark Current (I_{DC})	5 pA
Channel Noise Factor (Γ)	1.5
Photodiode Responsivity (R_p)	0.4 mA/mW
Equivalent Noise Bandwidth (B)	400 MHz
Open-Loop Voltage Gain (G)	10
Boltzmann's Constant (κ)	1.38×10^{-23}
Absolute Temperature (T_e)	300 K
Active Area (S)	.2 cm ²
Transconductance (g_m)	30 ms
Optical Filter Bandwidth ($\check{\lambda}$)	400 (380 – 780) nm
Spectral Irradiance (p_{BS})	5.8×10^{-6} W/cm ² ·nm
Photodiode Fixed Capacitance (η)	112 pF/cm ²
Interference (P_{diff})	0 W

and receiver and $\ell = \sqrt{d^2 - h^2}$. ℓ varies from 1 to 2 meters, and h varies from 1 to 3 meters. If the receiver is placed at a larger distance, $\sqrt{\text{CRLB}}$ will increase. More importantly, this figure represents that under the new model, the $\sqrt{\text{CRLB}}$ is higher than what was previously supposed. This considerable difference originates from the nature of VLC noise model, illustrating that RSN can't be ignored and has a significant effect on the theoretical accuracy analysis of VLP. As mentioned before, the other noise components are assumed to be more dominant in the literature. We emphasize that without solving the CRLB in detail, the relation between RSN and CRLB could not be found.

In Fig. 4, for several values of P_t , CRLB is plotted where it is assumed $m = 1$, ℓ varies from 1 to 2 meters, and h varies from 1 to 3 meters. Obviously,

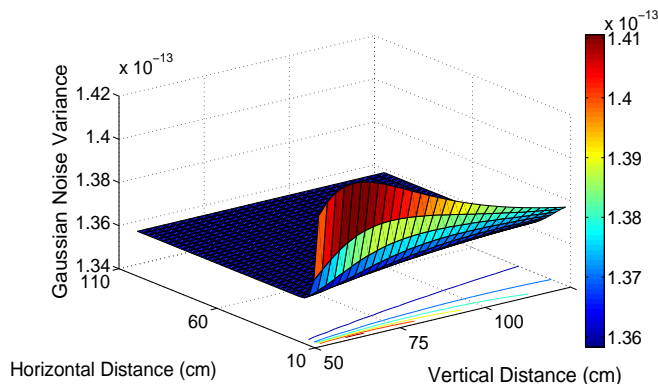


Figure 2: The influence on the variance of Gaussian noise of RSN for a typical room environment.

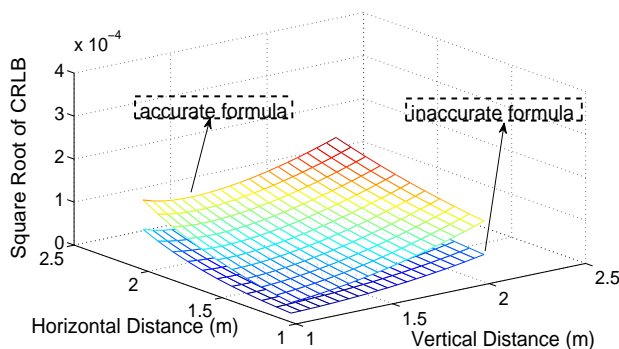


Figure 3: $\sqrt{\text{CRLB}}$ for proposed accurate formula by Equation (13) against inaccurate one (equation (16) of [20]) as a common formula in literature.

by increasing the transmitted optical power, the CRLB decreases toward lower values. More significantly, this figure shows that the relation between the transmitted optical power and the CRLB is so complicated. $\sqrt{\text{var}(\hat{d}_0)}$ is proportional to $\frac{1}{P_t}$ for lower values of received optical power, whereas for higher values of received optical power, $\sqrt{\text{var}(\hat{d}_0)}$ is proportional to $\frac{1}{\sqrt{P_t}}$. In other words, CRLB will decrease for higher values of received optical power. Although increasing the P_t is one way to rise the received optical power, eye safety regulations will limit the amount of transmitted optical power. However, received optical power

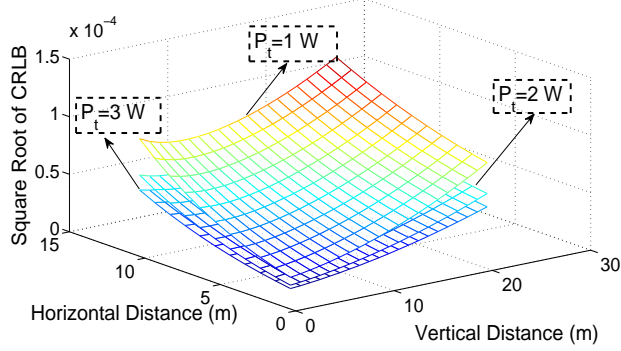


Figure 4: $\sqrt{\text{CRLB}}$ for proposed accurate formula by Equation (13) with several transmitted optical powers.

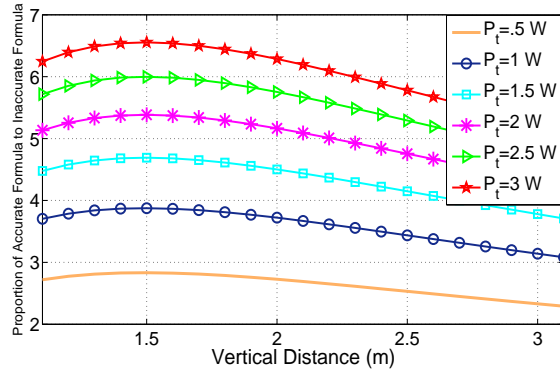


Figure 5: The proportion of accurate formula to inaccurate formula with several transmitted optical powers.

could be risen by some other ways such as increasing R_p or S , reducing d , and utilizing tilting technique.

The proportion of accurate formula of $\sqrt{\text{CRLB}}$ to inaccurate one is shown in Fig. 5. The figures present the mean of $\sqrt{\text{CRLB}}$ with regard to horizontal distance where $m = 1$, ℓ varies from 1 to 2 meters, and h varies from 1 to 3 meters. It can be clearly seen from Fig. 5 that the figures grow by increasing P_t . However, the rate of growth declines for higher values of transmitted optical power. This is because the impact of P_t on CRLB will decrease sharply for

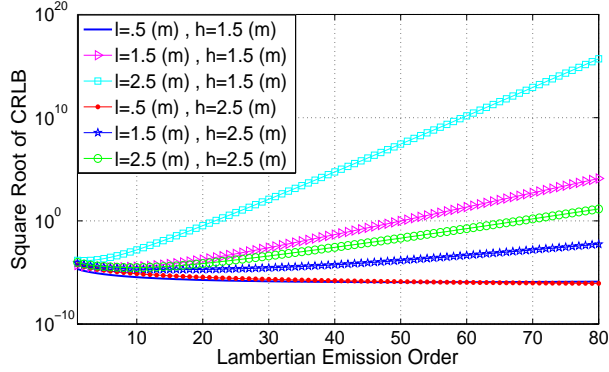


Figure 6: $\sqrt{\text{CRLB}}$ against the order of Lambertian emission with several values of horizontal distance and vertical distance.

higher values of received optical power. In addition, Fig. 5 illustrates that the relation between the transmitted optical power and the CRLB is complicated which should be discussed in the future.

In Fig. 6, the value of $\sqrt{\text{CRLB}}$ is evaluated by varying the horizontal distance and vertical distance. The radiation model of LEDs is not perfect Lambertian distribution in practical applications and m might be different in different LED manufacturers. We vary the value of m from 1 to 80. Fig. 6 indicates that by increasing horizontal distance for the given height, $\sqrt{\text{CRLB}}$ rises where $P_t = 1\text{W}$. Moreover, this figure shows that $\sqrt{\text{CRLB}}$ is a convex function, i.e. $\sqrt{\text{CRLB}}$ has a minimum value where $m = m_{\text{opt}}$. It is proved in [23] that $m_{\text{opt}} \approx -(2 + \frac{1}{\ln \cos \phi}) + \sqrt{1 + (\frac{1}{\ln \cos \phi})^2}$. In the future works, we would calculate m_{opt} more accurately.

5. Conclusion

For an indoor positioning system based on visible light, we have presented an analysis of the CRLB of RSS-based ranging. In this work, RSN is considered in modelling and showed that can not be negligible. By taking into account RSN and its relation to distance parameter, a more accurate noise model and closed-form expression for CRLB are achieved. A detailed discussion about the

parameters that determine the CRLB and their dependence on the geometry of the system is also presented. In addition, we have investigated the effect of Lambertian emission order on the $\sqrt{\text{CRLB}}$ and showed that $\sqrt{\text{CRLB}}$ is a convex function.

References

References

- [1] T.-H. Do and M. Yoo, An in-Depth Survey of Visible Light Communication Based Positioning Systems, *Sensors*, vol. 16, no. 5, pp. 678, 2016.
- [2] A. Naeem, N. U. Hassan, M. A. Pasha, C. Yuen, and A. Sikora, Performance analysis of TDOA-based indoor positioning systems using visible LED lights,” in *IEEE International Symposium on Wireless Systems within the International Conferences on Intelligent Data Acquisition and Advanced Computing Systems (IDAACS-SWS)*, 20–21 Sept. 2018, pp. 103–107, doi: 10.1109/IDAACS-SWS.2018.8525567.
- [3] X. Li, Y. Cao, and C. Chen, Machine learning based high accuracy indoor visible light location algorithm,” in *IEEE International Conference on Smart Internet of Things (SmartIoT)*, Aug. 2018, pp. 198–203.
- [4] A. Naz, N. U. Hassan, M. A. Pasha, H. Asif, T. M. Jadoon, and C. Yuen, Single LED ceiling lamp based indoor positioning system,” in *IEEE World Forum on Internet of Things (WF-IoT)*, Feb. 2018, pp. 682–687.
- [5] B. Ghimire, J. Seitz, and C. Mutschler, Indoor positioning using OFDM-based visible light communications systems,” in *International Conference on Indoor Positioning and Indoor Navigation (IPIN)*, Sep. 2018.
- [6] G. Shi, et al., Accuracy analysis of indoor visible light communication localization system based on received signal strength in non-line-of-sight environments by using least squares method, *Optical Engineering*, vol. 58, no. 5, pp. 1-11, May 2019.

- [7] S. Shen, S. Li and H. Steendam, Simultaneous Position and Orientation Estimation for Visible Light Systems With Multiple LEDs and Multiple PDs,” in *IEEE Journal on Selected Areas in Communications*, vol. 38, no. 8, pp. 1866-1879, Aug. 2020.
- [8] E. Gonendik and S. Gezici, Fundamental Limits on RSS Based Range Estimation in Visible Light Positioning Systems,” in *IEEE Communications Letters*, vol. 19, no. 12, pp. 2138–2141, Dec. 2015.
- [9] H. Steendam, T. Q. Wang, and J. Armstrong, Theoretical lower bound for indoor visible light positioning using received signal strength measurements and an aperture-based receiver,” *J. Lightw. Technol.*, vol. 35, no. 2, pp. 309–319, Jan. 2017.
- [10] N. Stevens and H. Steendam, Magnitude of the distance estimation bias in received signal strength visible light positioning, *IEEE Communications Letters*, vol. 22, no. 11, pp. 2250–2253, Nov. 2018.
- [11] P. Du, S. Zhang, C. Chen, A. Alphones, and W. Zhong, Demonstration of a low-complexity indoor visible light positioning system using an enhanced TDOA scheme, *IEEE Photonics Journal*, vol. 10, no. 4, pp. 1–10, Aug. 2018.
- [12] A. Sahin, Y. S. Eroglu, I. Guvenc, N. Pala, and M. Yuksel, Hybrid 3-D localization for visible light communication systems, *Journal of Lightwave Technology*, vol. 33, no. 22, pp. 4589–4599, Nov. 2015.
- [13] K. Panta and J. Armstrong, Indoor localization using white LEDs, *Electron. Lett.*, *IEEE* vol. 48, no. 4, pp. 228–230, Feb. 2012.
- [14] H. Manor and S. Arnon, Performance of an optical wireless communication system as a function of wavelength, *Appl. Opt.*, vol. 42, no. 21, pp. 4285–4294, Jul. 2003.
- [15] J. Wang, J. Wang, M. Chen and J. Wang, Capacity bounds for dimmable visible light communications using PIN photodiodes with input-dependent

- Gaussian noise,” 2014 IEEE Global Communications Conference, Austin, TX, 2014, pp. 2066-2071.
- [16] S. M. Moser, Capacity results of an optical intensity channel with input-dependent Gaussian noise, *IEEE Trans. Inf. Theory*, vol. 58, no. 1, pp. 207-223, Jan. 2012.
- [17] J. Gancarz, H. Elgala, and T. D. C. Little. Impact of lighting requirement on VLC systems, *IEEE Commun. Mag.*, vol. 51, no. 12, pp. 34–41, Dec. 2013.
- [18] Changeez Amini and Abbas Taherpour, Adaptive threshold device for detection of reflections based visible light communication, *Optics Communications*, vol. 388, pp. 1–11, 2017.
- [19] K. Lee and H. Park, Channel model and modulation schemes for visible light communications,” in *Proc. IEEE 54th Int. Midwest Symp. Circuits Syst.*, pp. 1–4, 2011.
- [20] X. Zhang, J. Duan, Y. Fu, and A. Shi, Theoretical accuracy analysis of indoor visible Light communication positioning system based on received signal strength indicator, *journal of Lightwave Technology*, vol. 32, no. 21, pp. 4180–4186, Nov. 2014.
- [21] T. Komine and M. Nakagawa, Fundamental analysis for visible-light communication system using LED lights, *IEEE Trans. Consumer Electron.*, vol. 50, no. 1, pp. 100–107, Feb. 2004.
- [22] Z. Ghassemlooy, W. Popoola, and S. Rajbhandari, *Optical Wireless Communications: System and Channel Modelling with MATLAB*, 2nd ed. CRC Press, May 2019.
- [23] C. Amini, A. Taherpour, T. Khattab, and S. Gazor, On the more accurate channel model and positioning based on time-of-arrival for visible light localization, *Opt. Eng.*, vol. 56, no. 1, pp. 1–12, 2017. [Online]. Available: <https://dx.doi.org/10.1117/1.OE.56.1.016110>